Design of Interdigital Bandpass Filters for Millimeter Wave Applications

Luis Alexandre S. Tapia, Elígia Simionato, Ivan Aldaya, José A. Oliveira and Rafael A. Penchel

***Abstract*— This work presents a third-order interdigital band-pass Butterworth filter designed to operate in the ISM band from 57 to 66 GHz. The project adopted an aluminum oxide (alumina) substrate, copper microstrip transmission lines and a coplanar waveguide (CPW) interface. We performed electromagnetic analysis in Ansys EM using the Finite Element Method (FEM). The filter presented return loss greater than 10 dB and insertion loss greater than 4.47 dB from 57.04 GHz to 65.45 GHz. We will fabricate the device using the Metallic-Nanowire-Membrane technology.**

***Keywords*— Millimeter waves, metallic-nanowire-membrane, interdigital filter**

I. Introduction

The growth in demand for data in every-day life lead to the search to enable use of new spectrum range, hence, the ISM (Industrial, Scientific, and Medical) spectrum range from 57 GHz to 66 GHz offers great advantages for short-distance wireless networks, such as high data transmission rates and great spatial isolation begotten by oxygen absorption peaks and high path-loss [1]. However, these features require manufacturing and integrating all elements of the RF system, i.e. transceiver, transmission lines, filters and antennas, in a System-on-Chip.

Regarding filter implementation, the use of lumped-element at millimeter wave (mmWave) frequencies is extremely difficult because the dimensions of the circuit elements (resistor, inductor, and capacitor) must be much smaller than the wavelength (λ = 5 mm at 60GHz) [2]. Distributed-element circuits approach can produce a similar behavior using $\lambda_g/4$ resonators, where $\lambda_g = \lambda/\sqrt{\epsilon_r}$. Even so, the resonators measure only a few millimeters ($R_L \sim 0.5$ mm for the alumina substrate), requiring advanced manufacturing techniques, like CMOS or BiCMOS [3].

The interdigital filter is a version of the hairpin filter that offers a good compromise between size and resonator Q-factor [4], where the quasi-TEM-mode transmission-line resonators are disposed in an array [5]. Each resonator has an open circuit and a short-circuit. Once the length of the hairpin line is $\lambda_g/2$, a virtual short circuit exists at the middle of the resonator. In the interdigital form, a real ground is used instead of a virtual one, as illustrated in Fig. 1. The whole structure is an array of transmission-line resonators, each one with an electrical length of $\lambda_g/4$. T_P is the electrical distance (in radians) between the tapping-point and the TSV (through-substrate via) short circuit; W_L and W_F represent the widths of the feed transmission line and the filter, respectively; and R_G indicates the gap between the filter elements.

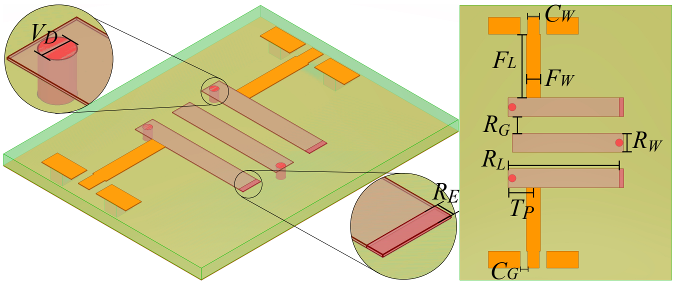

Fig. 1: Interdigital filter structure

Recently, an alternative process that uses an alumina substrate with Metallic-Nanowire-Membrane (MnM) demonstrates good results for 3D inductor, cross-overs, hybrids, antennas and other devices at millimeter waves frequencies [2]. This work aims to design and optimize a third-order interdigital band-pass filter with a pass-band from 57 to 66 GHz for manufacturing in MnM Technology. We performed the electromagnetic analysis in Ansys EM using the Finite Element Method (FEM) and used Aluminum oxide (alumina) as the substrate.

II. Interdigital Filter Design

To design the filter, we used the insertion loss method, that allows to manage the pass-band and stop-band amplitude and phase characteristics [6]. Then, to achieve a flat response in pass-band, a Butterworth frequency response was elected. A third-order filter was chosen to achieve a smaller-sized structure, with $f_L = 57$ GHz and $f_U = 66$ GHz as the lower and upper cutoff frequencies, respectively. First, the lumped-element filter was designed using equations described by [6]. The design is in Fig. 2 and values of inductors and capacitors are in Table I.

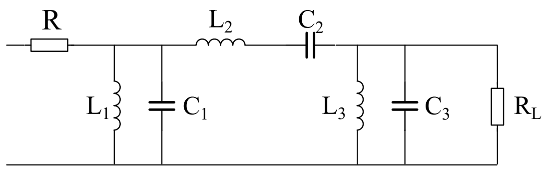

Fig. 2: Bandpass filter circuit

Luis Alexandre Silveira Tapia, FESJ/UNESP, São João da Boa Vista - SP, e-mail: luis.tapia@unesp.br; Elígia Simionato, FESJ/UNESP, São João da Boa Vista - SP, e-mail: e.simionato@unesp.br; Ivan Aldaya, FESJ/UNESP, São João da Boa Vista - SP, e-mail: ivan.aldaya@unesp.br; Rafael A. Penchel, FESJ/UNESP, São João da Boa Vista - SP, e-mail: rafael.penchel@unesp.br. This work was supported by the following Brazilian research agencies: FAPESP, grants #2022/02671-9, #2022/03519-6 and CNPq, grant #409146/2021-8

TABLE I: Values of lumped-element pass-band filter

Element	Abbreviation	Value
Input impedance	R	50 Ω
Load impedance	R_L	50 Ω
Capacitor 1	C_1	0.3537 pF
Capacitor 2	C_2	3.7871 fF
Capacitor 3	C_3	0.3537 pF
Inductor 1	L_1	18.9357 pH
Inductor 2	L_2	1.7683 nH
Inductor 3	L_3	18.9357 pH

Then, the design was implemented using distributed-elements. As shown in [5], the design procedure starts by computing the parameters

$$\theta = \frac{\pi}{2}\left(1 - \frac{\Delta f}{2f_o}\right) \quad \text{and} \quad Y = \frac{Y_o}{\tan\theta}\ , \tag{1}$$

where $\Delta f = f_U - f_L = 9$ GHz is the pass-band, $f_o = 61.5$GHz the central frequency and $Y_o = 1/Z_o$ is the input admittance ($Z_o = 50\Omega$). Furthermore, with an aluminum oxide (alumina) having a thickness of 50 μm, $\epsilon_r = 6.7$ and $\tan\delta = 0.015$ as the substrate and a 3 μm copper layer (used to simulate microstrip lines, ground, resonators, and coplanar waveguide interface), the resonator length ($R_L = 572$ μm), width ($R_W = 67$ μm) and gap ($R_G = 86.25$ μm) were determined. These dimensions were initially defined with help of the commercial software Advanced Design System (ADS) Keysight. The tapping-point distance ($T_P = 135$ μm) was got using the formulation presented in [5] and the through-substrate vias (TSV) were modeled as a copper cylinder. The structure and dimensions are shown in Fig. 1 and Table II, respectively.

TABLE II: Structure and dimensions: initial and final filter

Item	Dimensions	Size [μm] Initial project	Final project
Resonator's width	R_W	65	89
Resonator's length	R_L	572	525
Resonator extension length	R_E	0	21
Gap between resonators	R_G	86.25	79
Tap-point electrical length	T_P	135	120
Through-substrate-vias diameter	V_D	25	36
Feed-line length	F_L	300	300
Feed-line width	F_W	67	67
CPW width	C_W	55	55
CPW gap	C_G	35	35

III. Numerical Results

The reflection and transmission coefficients of the lumped-element circuit are shown in Fig. 3. The filter initial dimensions were analyzed using Ansys High-Frequency Structure Simulator (HFSS) module, which employs the Finite Element Method. It can be observed that the initial filter's behavior is close to the desired behavior, but the result is not satisfactory. To improve the filter frequency response, several parametric analyses were performed.

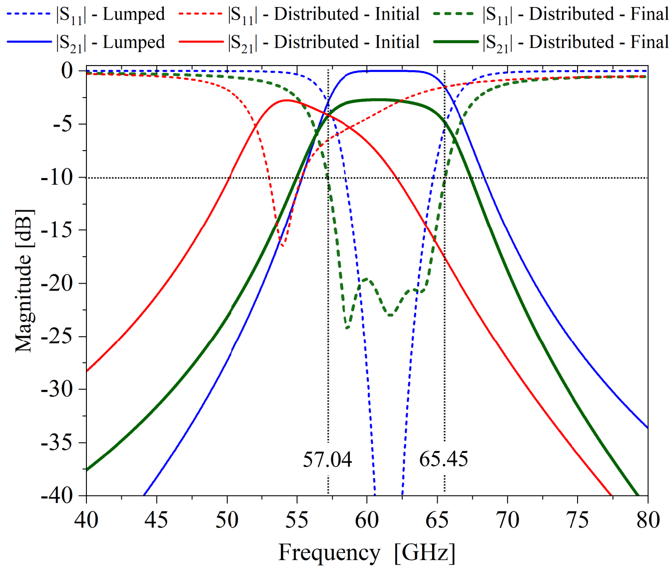

Fig. 3: Butterworth Filter design: lumped elements and distributed elements

It was observed that the size of the resonator controls the center frequency of operation, the tapping-point and the extension mainly affect the reflection coefficient and the resonator gap affects the pass-band. The optimization process leads to the final dimensions in Table II. The reflection and transition coefficients presented in Fig. 3 are close to what was initially expected.

IV. Conclusions

The proposed third-order interdigital Butterworth filter design achieved $|S_{11}| \leq -10$ dB for frequencies between 57.04 GHz and 65.45 GHz, corresponding to the regulated ISM band. Also, the implementation of extensions, a better position for tapping-point and modifications in the resonator gap enabled a superior impedance matching, therefore, $|S_{21}| = -2.711$ dB was achieved at the central frequency. The pass-band of the final distributed-elements design is wider than the lumped-element circuit, although the $|S_{21}|$ is of higher quality on the second case. That shows the proposed filter, with alumina as substrate, can be an alternative to be considered compared to other technologies.

References

[1] M. Marcus and B. Pattan, "Millimeter wave propagation: spectrum management implications," *IEEE Microwave Magazine*, vol. 6, no. 2, pp. 54–62, Jun. 2005.

[2] J. E. G. Lé, M. Ouvrier-Buffet, L. G. Gomes, R. A. Penchel, A. L. C. Serrano, and K. G. P. Rehder, "Integrated Antennas on MnM Interposer for the 60 GHz Band," *Journal of Microwaves, Optoelectronics and Electromagnetic Applications*, vol. 21, pp. 184–193, Mar. 2022. [Online]. Available: http://www.scielo.br/j/jmoea/a/Zm95w4WLFKVYp3cmZGjPJQJ/

[3] R. Karim, A. Iftikhar, and R. Ramzan, "Performance-issues-mitigation-techniques for on-chip-antennas – recent developments in rf, mm-wave, and thz bands with future directions," *IEEE Access*, vol. 8, pp. 219 577–219 610, 2020.

[4] P. Pramanick and P. Bhartia, *Modern RF and microwave filter design*. Artech House, 2016.

[5] J.-S. Hong, *Microstrip filters for RF/Microwave Applications*. Wiley, 2011.

[6] D. M. Pozar, *Microwave engineering*, 4th ed. Wiley, 2012.